

Linear scaling of lepton charge asymmetry in W^\pm production in ultra-relativistic nuclear collisions

An-Ke Lei,¹ Dai-Mei Zhou,^{1,*} Yu-Liang Yan,^{2,†} Xiao-Ming Zhang,¹ Liang Zheng,³
 Du-Juan Wang,⁴ Xiao-Mei Li,² Gang Chen,³ Xu Cai,¹ and Ben-Hao Sa^{1,2,‡}

¹*Key Laboratory of Quark and Lepton Physics (MOE) and Institute of Particle Physics,
 Central China Normal University, Wuhan, 430079, China*

²*China Institute of Atomic Energy, P. O. Box 275 (10), Beijing, 102413, China*

³*School of Mathematics and Physics, China University of Geosciences (Wuhan), Wuhan 430074, China*

⁴*Department of Physics, Wuhan University of Technology, Wuhan 430070, China*

(Dated: October 25, 2022)

The lepton charge asymmetry in W^\pm production in the nuclear collisions at $\sqrt{s_{NN}} = 5.02$ TeV is investigated with a parton and hadron cascade model PACIAE. Recently published ALICE and the ATLAS data of lepton charge asymmetry are well reproduced. An interesting linear scaling behavior is observed in the lepton charge asymmetry as a function of the collision system valence quark number asymmetry among the different size of nuclear collision systems at $\sqrt{s_{NN}} = 5.02$ TeV. This linear scaling behavior may serve as an additional constraint on the PDF (nPDF) extractions.

I. INTRODUCTION

W^\pm vector bosons are heavy particles with masses of $m_{W^\pm} \approx 80$ GeV/ c^2 [1, 2]. They are mainly produced in the hard partonic scattering processes with large momentum transfer at the early stage of the (ultra-)relativistic nuclear collisions. In comparison with evolution time of the heavy-ion collision system, 10 to 100 fm/ c for instance, the W^\pm decay time (~ 0.0922 fm/ c , estimated with full decay width, $t = h/\Gamma$ [1]) is very short. The W^\pm leptonic decays

$$W^\pm \rightarrow l^\pm \nu_l, \quad (l: e, \mu, \tau)$$

are nearly instantaneous. As the produced leptons weakly interact with the partonic and hadronic matter created in nuclear collisions, the W^\pm is a powerful probe for investigating the properties of the initial state in the nuclear collision system. The main production processes of W^\pm are

$$u\bar{d} \rightarrow W^+, \quad d\bar{u} \rightarrow W^-$$

in the leading-order (LO) approximation [1, 3]. With the involvement of the valence u - and d -quarks inside the nuclear system, the isospin difference between proton and neutron is important for the production of W^+ and W^- . It is therefore expected that the W^\pm boson charge asymmetry and the corresponding decayed lepton charge asymmetry are related to the relative abundance of protons and neutrons (to the relative abundance of valence u - and d -quarks) of the collision system. The lepton charge asymmetry A_l could be defined as the difference between the multiplicity of positive and negative leptons

divided by their sum:

$$A_l = \frac{N_{l^+ \leftarrow W^+} - N_{l^- \leftarrow W^-}}{N_{l^+ \leftarrow W^+} + N_{l^- \leftarrow W^-}}. \quad (1)$$

Similarly, the collision system valence u (d) quark number asymmetry A_v is defined as

$$A_v = \frac{N_u - N_d}{N_u + N_d}, \quad (2)$$

where N_u (N_d) refers to the number of valence quark u (d) in the nuclear collision system.

The lepton charge asymmetry have been measured in $p\bar{p}$ collisions at $\sqrt{s} = 1.8$ and 1.96 TeV by CDF [4–8] and D0 [9–11] collaborations on Fermilab Tevatron. They give early complementary constrains on Parton Distribution Function (PDF) relative to the deep inelastic scattering experiments. More precise measurements in pp collisions at $\sqrt{s}=7$ and 8 TeV are reported by ATLAS [12–15], CMS [16–20] and LHCb [21–24] collaborations on the Large Hadron Collider (LHC) at CERN. ATLAS also give the measurements in pp collisions at $\sqrt{s} = 2.76$ [25] and 5.02 TeV [26]. Beyond the elementary pp collisions, the lepton charge asymmetry has been measured in the p+Pb collisions at $\sqrt{s_{NN}} = 5.02$ TeV by ALICE [27] and at $\sqrt{s_{NN}} = 8.16$ TeV by ALICE [28] and CMS [29]. The results of lepton charge asymmetry in Pb+Pb collisions at $\sqrt{s_{NN}} = 2.76$ TeV are first given by ATLAS [30] and CMS [18]. Recently, ATLAS and ALICE published their results of W^\pm production cross-section and lepton charge asymmetry in Pb+Pb collisions at $\sqrt{s_{NN}} = 5.02$ TeV [28, 31]. All those measurements are declared to be well reproduced by the LO and/or next-to-leading-order (NLO) perturbative Quantum Chromodynamics (pQCD) calculations [32–35] using the CT14 PDF set [32] with or without the nuclear modified PDF (nPDF).

In this paper, the parton and hadron cascade model PACIAE [36] is employed to reproduce the ATLAS and ALICE lepton charge asymmetry data in Pb+Pb at

* zhoum@mail.cnu.edu.cn

† yanyl@ciae.ac.cn

‡ sabh@ciae.ac.cn

$\sqrt{s_{\text{NN}}} = 5.02$ TeV [28, 31]. We then calculate the lepton charge asymmetry as a function of the collision system valence quark number asymmetry in both the elementary nucleon-nucleon (NN) and the nucleus-nucleus (AA) collisions at $\sqrt{s_{\text{NN}}} = 5.02$ TeV. An interesting linear scaling behavior in the lepton charge asymmetry as the function of collision system valence quark number asymmetry is observed among the different NN and AA collision systems.

The paper is organized as follows. In Sec. II, we describe the PACIAE model and the setups for W^\pm production in PYTHIA 6.4, with a precision equivalent to the NLO pQCD. The simulated results and discussions are presented in Sec. III. At last, a summary is given in Sec. IV.

II. MODEL

A parton and hadron cascade model PACIAE [36] is employed to simulate the elementary nucleon-nucleon (NN: pp , pn , np and nn) and the nucleus-nucleus (AA: Cu+Cu, Xe+Xe, Au+Au, Pb+Pb and U+U) collisions at $\sqrt{s_{\text{NN}}} = 5.02$ TeV.

The PACIAE model is based on PYTHIA event generator (version 6.4.28) [37]. For NN collisions, with respect to PYTHIA, the partonic and hadronic rescatterings are introduced before and after the hadronization, respectively. The final hadronic state is developed from the initial partonic hard scattering and parton showers, followed by parton rescattering, string fragmentation, and hadron rescattering stages. Thus, the PACIAE model provides a multi-stage transport description on the evolution of the NN collision system.

For AA collisions, the initial positions of nucleons in the colliding nucleus are sampled according to the Woods-Saxon distribution. Together with the initial momentum setup of $p_x = p_y = 0$ and $p_z = p_{\text{beam}}$ for each nucleon, a list containing the initial state of all nucleons in a given AA collision is constructed. A collision happened between two nucleons from different nuclei if their relative transverse distance is less than or equal to the minimum approaching distance: $D \leq \sqrt{\sigma_{\text{NN}}^{\text{tot}}/\pi}$. The collision time is calculated with the assumption of straight-line trajectories. All such nucleon pairs compose an NN collision time list. An NN collision with least collision time is selected from the list and executed by PYTHIA (PYEVNW subroutine) with the hadronization temporarily turned-off, as well as the strings and diquarks broken-up. The nucleon list and NN collision time list are then updated. A new NN collision with least collision time is selected from the updated NN collision time list and executed by PYTHIA. With repeating the aforementioned steps till the NN collision list empty, the initial partonic state is constructed for a AA collision.

Then, the partonic rescatterings are performed, where the LO-pQCD parton-parton cross section [38, 39] is employed. After partonic rescattering, the string is recov-

ered and then hadronized with the Lund string fragmentation scheme resulting in an intermediate hadronic state. Finally, the system proceeds into the hadronic rescattering stage and produces the final hadronic state observed in the experiments.

The PACIAE Monte-Carlo simulation provides a complete description of the NN and AA collisions, which includes the partonic initialization, partonic rescattering, hadronization, and the hadronic rescattering stages. Meanwhile, a PACIAE model simulation could be selected to stop at any stage desired conveniently. In this work, the simulations are stopped at the partonic initialization stage, after the initial hard scattering and parton shower processes happened.

In this study, the W^\pm relevant production channels are activated in a user-controlled approach by setting $\text{MSEL} = 0$ in PYTHIA, together with the following subprocesses switched-on:

$$\begin{aligned} f_i \bar{f}_j &\rightarrow W^+ / W^-, \\ f_i \bar{f}_j &\rightarrow gW^+ / W^-, \\ f_i \bar{f}_j &\rightarrow \gamma W^+ / W^-. \end{aligned}$$

In the above equations, f refers to fermions (quarks) and its subscript stands for the flavor code.

In addition, the parton shower is switched off by setting $\text{MSTP}(61)=0$ and $\text{MSTP}(71)=0$, to prevent the double-counting. The PDF and other parameters are kept the same as the default PYTHIA. Thus the PACIAE (PYTHIA) model simulation is corresponding to the NLO pQCD in precision.

III. RESULTS AND DISCUSSIONS

In the left panel of Fig. 1, we compare the PACIAE model calculated electron and muon combined lepton charge asymmetry (black solid squares) with ATLAS data [31] (red solid circles) for the 0-80% centrality class in Pb+Pb collisions at $\sqrt{s_{\text{NN}}} = 5.02$ TeV. The bottom sub-panel shows the differences between PACIAE calculation and ATLAS data, where the shaded boxes show the total uncertainties experimental data. The kinematic cuts in PACIAE simulation is the same as the ones in ATLAS experiments [31], i.e.

$$\begin{aligned} p_T^l &> 25 \text{ GeV}/c, & p_T^\nu &> 25 \text{ GeV}/c, \\ |\eta_l| &< 2.5, & m_T &> 40 \text{ GeV}/c^2, \end{aligned}$$

where p_T^l and p_T^ν stand for the transverse momentum of the lepton and the corresponding neutrino, respectively. $|\eta_l|$ refers to the absolute pseudorapidity of the lepton, and m_T is the transverse mass of the lepton and neutrino system. The pseudorapidity bins are divided as follows:

$$\begin{aligned} |\eta_l| = & (0, 0.21), & (0.21, 0.42), & (0.42, 0.63), & (0.63, 0.84), \\ & (0.84, 1.05), & (1.05, 1.37), & (1.37, 1.52), & (1.52, 1.74), \\ & (1.74, 1.95), & (1.95, 2.18), & (2.18, 2.5). \end{aligned}$$

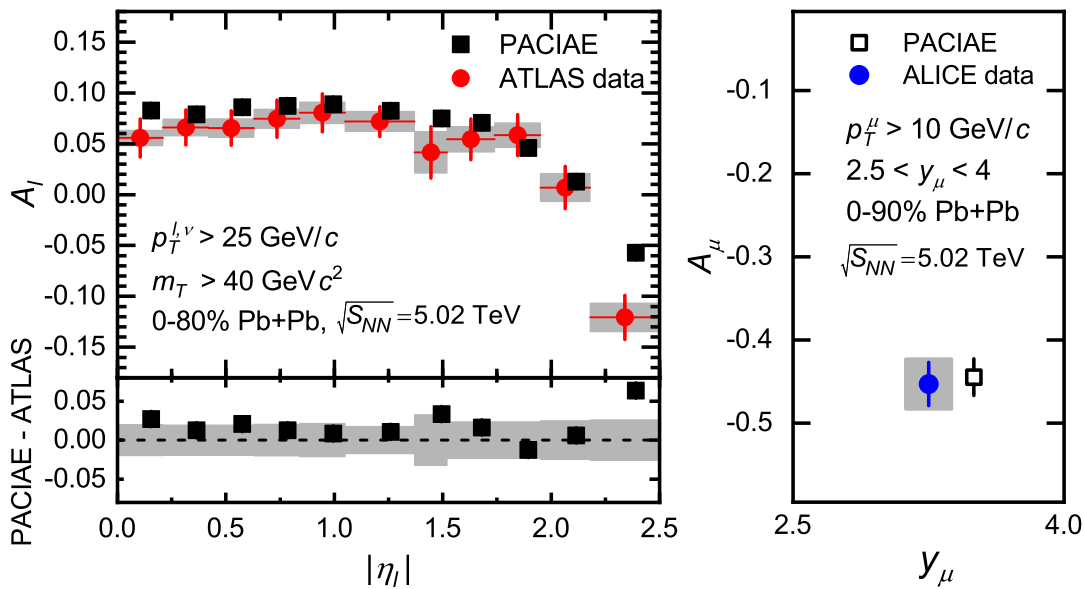


FIG. 1. Left panel: the combined electron and muon charge asymmetry as a function of absolute pseudorapidity for the 0-80% centrality class in Pb+Pb collisions at $\sqrt{s_{NN}} = 5.02 \text{ TeV}$. The black solid squares with vertical error bar (hard to see) show the results of PACIAE simulations. The red solid circles with vertical error bars and shaded error boxes represent the ATLAS data [31]. The lower sub-panel shows the differences between the PACIAE calculations and the ATLAS data, with the shaded boxes representing the total experimental uncertainties. The PACIAE result points are shifted horizontally for better visibility. Right panel: the muon charge asymmetry for the 0-90% centrality class in Pb+Pb collisions at $\sqrt{s_{NN}} = 5.02 \text{ TeV}$, with kinematic cuts of $p_T^\mu > 10 \text{ GeV}/c$ and $2.5 < y_\mu < 4.0$. Here the open square with vertical error bar shows the result of PACIAE simulation, and the blue solid circle with vertical error bar and shaded error box represents ALICE datum [28].

We see in this panel, the PACIAE calculated lepton charge asymmetry is well consistent with ATLAS data [31], except the most forward $|\eta|$ bin. This exception is also existed in the pQCD predictions calculated with the CT14 NLO PDF set, even in the EPPS16 and nCTEQ15 nPDF sets [31].

The PACIAE calculation of the muon charge asymmetry (open square) for the 0-90% centrality class in Pb+Pb collisions at $\sqrt{s_{NN}} = 5.02 \text{ TeV}$ is compared with the ALICE datum [28] (blue solid circle) in the right panel of Fig. 1. The same kinematic cuts of $p_T^\mu > 10 \text{ GeV}/c$ and $2.5 < y_\mu < 4$ [40] are set in both the experiment and theory. One can see in this panel that, the calculated result agrees well with the ALICE datum.

In Fig. 2, we give the muon charge asymmetry as a function of the valence quark number asymmetry in the elementary NN collisions of pp (open triangle-ups), pn (triangle-left), np (triangle-right), and nn (triangle-downs)

at $\sqrt{s} = 5.02 \text{ TeV}$. The kinematic cut of $p_T^\mu > 10 \text{ GeV}/c$ is implemented in the simulations for three y_μ intervals: $|y_\mu| < 1$, $2.5 < |y_\mu| < 4.0$, and full y_μ phase-space. The dashed, dotted and dash-dotted lines represent the linear fitting to the function of A_μ vs. A_v in three y_μ intervals above, respectively. One can see all of A_μ in pp , pn , np and nn collisions are positive in mid-rapidity ($|y_\mu| < 1$), while negative in the forward rapidity ($2.5 < |y_\mu| < 4$). This sign-changing phenomenon has been also observed in LHCb measurements [21–24]. It comes from the dif-

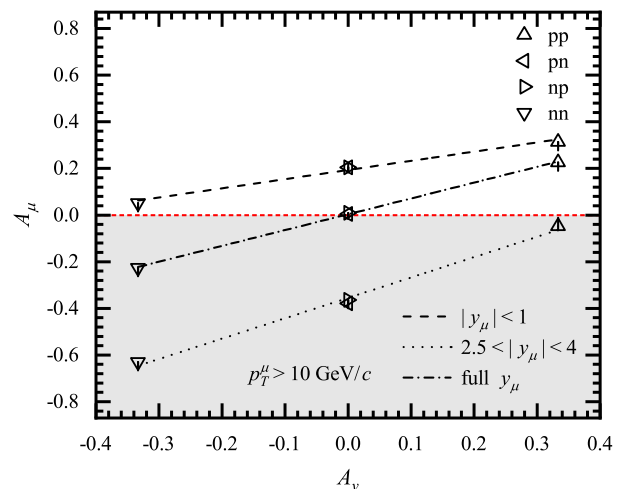


FIG. 2. The muon charge asymmetry as a function of the valence quark asymmetry in the elementary NN collisions (pp , open triangle-ups; pn , open triangle-left; np , open triangle-right; and nn , open triangle-downs) at $\sqrt{s} = 5.02 \text{ TeV}$ for three rapidity intervals of $|y| < 1$, $2.5 < |y| < 4.0$, and full rapidity phase-space. The dashed, dotted, and dash-dotted lines are the corresponding linear fitting to the A_μ vs. A_v functions, respectively. The kinematic cut is $p_T^\mu > 10 \text{ GeV}/c$. The red short-dashed zero-baseline and the shaded area are added for better distinguishment between the positive and negative values of A_μ .

ferent helicity dependence of the lepton couplings to the boson [21]. For full rapidity phase-space, A_μ in pn and np collisions is consistent with zero owing to the vanishing relative numbers between u - and d -valence quarks, while the A_μ in pp and nn are almost equal in magnitude but opposite in sign. On the other hand, we can see the slope fitted in mid-rapidity is gentler than the one in the forward rapidity, due to the isospin effect in W^\pm production is more pronounced at forward rapidity [41].

The correlation between A_μ and A_v in symmetrical AA collisions of Cu+Cu (solid circles), Xe+Xe (solid squares), Au+Au (solid stars), Pb+Pb (solid pentagons) and U+U (solid diamonds) at $\sqrt{s_{NN}} = 5.02$ TeV for three rapidity intervals is shown in Fig. 3, with the kinematic cut of $p_T^\mu > 10$ GeV/c. The corresponding linear fitting is also given. In this figure, the valence quark number asymmetry (A_v) are all negative, since the number of neutrons (the number of d quarks) is always greater than that of protons (u quarks) in heavy nuclei. The A_μ is positive in the mid-rapidity bin for all five AA collision systems but negative in the forward and full rapidity regions. It can be attributed to the $V - A$ decays of W boson. This structure also affects the slope of the linear fitting. With the ratio of neutron to proton (A_v magnitude) increasing, the fraction of $W^- \rightarrow l^- \nu_l$ becomes larger in forward rapidity resulting a steeper slope than the one in mid-rapidity [21, 41]. It is more clear in Fig. 4, where we draw the A_μ vs. A_v function in all the NN and AA collisions together. Here we see the fitted slope in the full rapidity is larger than the one in mid-rapidity, but is smaller than that in forward rapidity. One more interesting feature is that, the linear scaling behavior of A_μ vs. A_v shown in Fig. 2 is also observed in Fig. 3 and 4.

IV. SUMMARY

In summary, we studied the lepton charge asymmetry from the W^\pm decays in both the NN and AA nuclear collisions at $\sqrt{s_{NN}} = 5.02$ TeV in frame of the Monte-Carlo simulation model PACIAE. The simulated results well reproduce the corresponding ATLAS and ALICE data. Furthermore, the correlation between the lepton charge asymmetry A_μ and the valence quark number asymmetry A_v is studied in the above nuclear collisions for three rapidity intervals: $|y_\mu| < 1$, $2.5 < |y_\mu| < 4$, and the full rapidity phase space. In each rapidity interval, a linear scaling behavior of A_μ vs. A_v function is observed in the elementary NN collision systems (pp , pn , np , and nn), the AA collision systems (Cu+Cu, Xe+Xe, Au+Au, Pb+Pb, and U+U), and even in their combination.

The universal linear scaling behavior between A_μ and A_v explored in both nucleon-nucleon and nucleus-nucleus collision systems may provide an additional constraint in the extraction of PDF (nPDF). On the contrary, we also note that the nuclear modifications on the vacuum nucleon PDF change the in-going parton kinematics in the hard scattering processes and consequently impact the

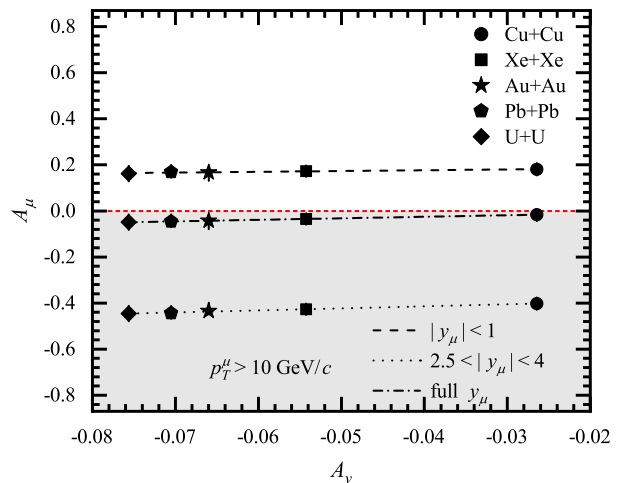


FIG. 3. The muon charge asymmetry as a function of the valence quark number asymmetry in the symmetric AA collisions (Cu+Cu, solid circles; Xe+Xe, solid squares; Au+Au, solid stars; Pb+Pb, solid pentagons; and U+U, solid diamonds) at $\sqrt{s_{NN}} = 5.02$ TeV for three rapidity intervals of $|y_\mu| < 1$, $2.5 < |y_\mu| < 4.0$, and full rapidity phase-space. The dashed, dotted and dash-dotted lines are the corresponding linear fitting to the A_μ vs. A_v functions, respectively. The kinematic cut is $p_T^\mu > 10$ GeV/c. The red short-dashed zero-baseline and the shaded area are added for better distinguishment between the positive and negative values of A_μ .

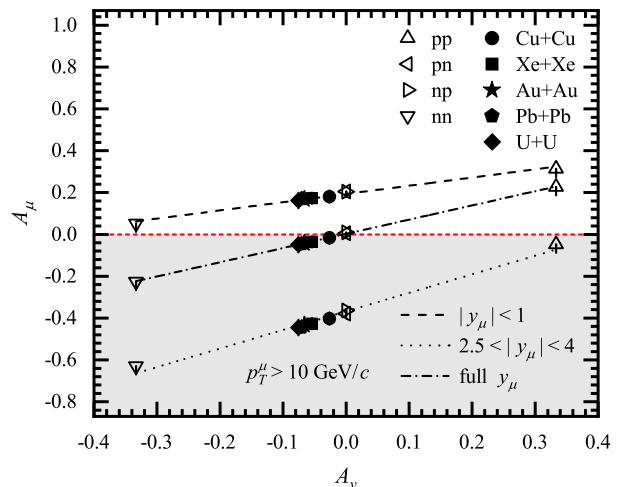


FIG. 4. The muon charge asymmetry as a function of the valence quark number asymmetry in the elementary NN collisions and the symmetric AA collisions at $\sqrt{s_{NN}} = 5.02$ TeV, obtained by putting Fig. 2 and 3 together.

p_T - and y -distribution of the out-going particles. This effect should result in a breaking of the A_μ vs. A_v scaling established if looking into a given lepton p_T - y phase space. Therefore, by measuring p_T and y differentially, the deviation of the A_μ vs. A_v correlations between NN and AA collision systems should provide a new tool to constrain the nPDF in a wide Bjorken- x region. This has to be studied further.

ACKNOWLEDGMENTS

The authors thank helpful discussion with Ming-Rui Zhao. This work was supported by the National Natural Science Foundation of China (11775094, 11805079,

11905188, 11775313, 11905163), the Continuous Basic Scientific Research Project (No.WDJC-2019-16) in CIAE, National Key Research and Development Project (2018YFE0104800) and by the 111 project of the foreign expert bureau of China.

-
- [1] P. A. Zyla *et al.* (Particle Data Group), Review of Particle Physics, *PTEP* **2020**, 083C01 (2020).
- [2] T. Aaltonen *et al.* (CDF), High-precision measurement of the W boson mass with the CDF II detector, *Science* **376**, 170 (2022).
- [3] A. D. Martin, R. G. Roberts, W. J. Stirling, and R. S. Thorne, Parton distributions and the LHC: W and Z production, *Eur. Phys. J. C* **14**, 133 (2000), [arXiv:hep-ph/9907231](#).
- [4] F. Abe *et al.* (CDF), Lepton asymmetry in W decays from $p\bar{p}$ collisions at $\sqrt{s} = 1.8$ TeV, *Phys. Rev. Lett.* **68**, 1458 (1992).
- [5] F. Abe *et al.* (CDF), The Charge asymmetry in W boson decays produced in $p\bar{p}$ collisions at $\sqrt{s} = 1.8$ TeV, *Phys. Rev. Lett.* **74**, 850 (1995), [arXiv:hep-ex/9501008](#).
- [6] F. Abe *et al.* (CDF), Measurement of the Lepton Charge Asymmetry in W Boson Decays Produced in $p\bar{p}$ Collisions, *Phys. Rev. Lett.* **81**, 5754 (1998), [arXiv:hep-ex/9809001](#).
- [7] D. Acosta *et al.* (CDF), Measurement of the forward-backward charge asymmetry from $W \rightarrow e\nu$ production in $p\bar{p}$ collisions at $\sqrt{s} = 1.96$ TeV, *Phys. Rev. D* **71**, 051104 (2005), [arXiv:hep-ex/0501023](#).
- [8] T. Aaltonen *et al.* (CDF), Direct Measurement of the W Production Charge Asymmetry in $p\bar{p}$ Collisions at $\sqrt{s} = 1.96$ TeV, *Phys. Rev. Lett.* **102**, 181801 (2009), [arXiv:0901.2169 \[hep-ex\]](#).
- [9] V. M. Abazov *et al.* (D0), Measurement of the muon charge asymmetry from W boson decays, *Phys. Rev. D* **77**, 011106 (2008), [arXiv:0709.4254 \[hep-ex\]](#).
- [10] V. M. Abazov *et al.* (D0), Measurement of the electron charge asymmetry in $p\bar{p} \rightarrow W + X \rightarrow e\nu + X$ events at $\sqrt{s} = 1.96$ -TeV, *Phys. Rev. Lett.* **101**, 211801 (2008), [arXiv:0807.3367 \[hep-ex\]](#).
- [11] V. M. Abazov *et al.* (D0), Measurement of the Muon Charge Asymmetry in $p\bar{p} \rightarrow W+X \rightarrow \mu\nu + X$ Events at $\sqrt{s}=1.96$ TeV, *Phys. Rev. D* **88**, 091102 (2013), [arXiv:1309.2591 \[hep-ex\]](#).
- [12] G. Aad *et al.* (ATLAS), Measurement of the W charge asymmetry in the $W \rightarrow \mu\nu$ decay mode in pp collisions at $\sqrt{s} = 7$ TeV with the ATLAS detector, *Phys. Lett. B* **701**, 31 (2011), [arXiv:1103.2929 \[hep-ex\]](#).
- [13] G. Aad *et al.* (ATLAS), Measurement of the inclusive W^\pm and Z/γ cross sections in the electron and muon decay channels in pp collisions at $\sqrt{s} = 7$ TeV with the ATLAS detector, *Phys. Rev. D* **85**, 072004 (2012), [arXiv:1109.5141 \[hep-ex\]](#).
- [14] M. Aaboud *et al.* (ATLAS), Precision measurement and interpretation of inclusive W^+ , W^- and Z/γ^* production cross sections with the ATLAS detector, *Eur. Phys. J. C* **77**, 367 (2017), [arXiv:1612.03016 \[hep-ex\]](#).
- [15] G. Aad *et al.* (ATLAS), Measurement of the cross-section and charge asymmetry of W bosons produced in proton–proton collisions at $\sqrt{s} = 8$ TeV with the ATLAS detector, *Eur. Phys. J. C* **79**, 760 (2019), [arXiv:1904.05631 \[hep-ex\]](#).
- [16] S. Chatrchyan *et al.* (CMS), Measurement of the Inclusive W and Z Production Cross Sections in pp Collisions at $\sqrt{s} = 7$ TeV, *JHEP* **10**, 132, [arXiv:1107.4789 \[hep-ex\]](#).
- [17] S. Chatrchyan *et al.* (CMS), Measurement of the Electron Charge Asymmetry in Inclusive W Production in pp Collisions at $\sqrt{s} = 7$ TeV, *Phys. Rev. Lett.* **109**, 111806 (2012), [arXiv:1206.2598 \[hep-ex\]](#).
- [18] S. Chatrchyan *et al.* (CMS), Study of W boson production in PbPb and pp collisions at $\sqrt{s_{NN}} = 2.76$ TeV, *Phys. Lett. B* **715**, 66 (2012), [arXiv:1205.6334 \[nucl-ex\]](#).
- [19] S. Chatrchyan *et al.* (CMS), Measurement of the Muon Charge Asymmetry in Inclusive $pp \rightarrow W + X$ Production at $\sqrt{s} = 7$ TeV and an Improved Determination of Light Parton Distribution Functions, *Phys. Rev. D* **90**, 032004 (2014), [arXiv:1312.6283 \[hep-ex\]](#).
- [20] V. Khachatryan *et al.* (CMS), Measurement of the differential cross section and charge asymmetry for inclusive $pp \rightarrow W^\pm + X$ production at $\sqrt{s} = 8$ TeV, *Eur. Phys. J. C* **76**, 469 (2016), [arXiv:1603.01803 \[hep-ex\]](#).
- [21] R. Aaij *et al.* (LHCb), Inclusive W and Z production in the forward region at $\sqrt{s} = 7$ TeV, *JHEP* **06**, 058, [arXiv:1204.1620 \[hep-ex\]](#).
- [22] R. Aaij *et al.* (LHCb), Measurement of the forward W boson cross-section in pp collisions at $\sqrt{s} = 7$ TeV, *JHEP* **12**, 079, [arXiv:1408.4354 \[hep-ex\]](#).
- [23] R. Aaij *et al.* (LHCb), Measurement of forward W and Z boson production in pp collisions at $\sqrt{s} = 8$ TeV, *JHEP* **01**, 155, [arXiv:1511.08039 \[hep-ex\]](#).
- [24] R. Aaij *et al.* (LHCb), Measurement of forward $W \rightarrow e\nu$ production in pp collisions at $\sqrt{s} = 8$ TeV, *JHEP* **10**, 030, [arXiv:1608.01484 \[hep-ex\]](#).
- [25] G. Aad *et al.* (ATLAS), Measurement of W^\pm -boson and Z -boson production cross-sections in pp collisions at $\sqrt{s} = 2.76$ TeV with the ATLAS detector, *Eur. Phys. J. C* **79**, 901 (2019), [arXiv:1907.03567 \[hep-ex\]](#).
- [26] M. Aaboud *et al.* (ATLAS), Measurements of W and Z boson production in pp collisions at $\sqrt{s} = 5.02$ TeV with the ATLAS detector, *Eur. Phys. J. C* **79**, 128 (2019), [Erratum: *Eur.Phys.J.C* **79**, 374 (2019)], [arXiv:1810.08424 \[hep-ex\]](#).
- [27] J. Adam *et al.* (ALICE), W and Z boson production in p–Pb collisions at $\sqrt{s_{NN}} = 5.02$ TeV, *JHEP* **02**, 077, [arXiv:1611.03002 \[nucl-ex\]](#).
- [28] ALICE collaboration, W^\pm -boson production in p–Pb collisions at $\sqrt{s_{NN}} = 8.16$ TeV and PbPb collisions at $\sqrt{s_{NN}} = 5.02$ TeV, [arXiv:2204.10640 \[nucl-ex\]](#).

- [29] A. M. Sirunyan *et al.* (CMS), Observation of nuclear modifications in W^\pm boson production in pPb collisions at $\sqrt{s_{NN}} = 8.16$ TeV, *Phys. Lett. B* **800**, 135048 (2020), [arXiv:1905.01486 \[hep-ex\]](#).
- [30] G. Aad *et al.* (ATLAS), Measurement of the production and lepton charge asymmetry of W bosons in Pb+Pb collisions at $\sqrt{s_{NN}} = 2.76$ TeV with the ATLAS detector, *Eur. Phys. J. C* **75**, 23 (2015), [arXiv:1408.4674 \[hep-ex\]](#).
- [31] G. Aad *et al.* (ATLAS), Measurement of W^\pm boson production in Pb+Pb collisions at $\sqrt{s_{NN}} = 5.02$ TeV with the ATLAS detector, *Eur. Phys. J. C* **79**, 935 (2019), [arXiv:1907.10414 \[nucl-ex\]](#).
- [32] S. Dulat, T.-J. Hou, J. Gao, M. Guzzi, J. Huston, P. Nadolsky, J. Pumplin, C. Schmidt, D. Stump, and C. P. Yuan, New parton distribution functions from a global analysis of quantum chromodynamics, *Phys. Rev. D* **93**, 033006 (2016), [arXiv:1506.07443 \[hep-ph\]](#).
- [33] K. J. Eskola, H. Paukkunen, and C. A. Salgado, EPS09: A New Generation of NLO and LO Nuclear Parton Distribution Functions, *JHEP* **04**, 065, [arXiv:0902.4154 \[hep-ph\]](#).
- [34] A. Kusina, F. Lyonnet, D. B. Clark, E. Godat, T. Jezo, K. Kovarik, F. I. Olness, I. Schienbein, and J. Y. Yu, Vector boson production in pPb and PbPb collisions at the LHC and its impact on nCTEQ15 PDFs, *Eur. Phys. J. C* **77**, 488 (2017), [arXiv:1610.02925 \[nucl-th\]](#).
- [35] K. J. Eskola, P. Paakkinen, H. Paukkunen, and C. A. Salgado, EPPS16: Nuclear parton distributions with LHC data, *Eur. Phys. J. C* **77**, 163 (2017), [arXiv:1612.05741 \[hep-ph\]](#).
- [36] B.-H. Sa, D.-M. Zhou, Y.-L. Yan, X.-M. Li, S.-Q. Feng, B.-G. Dong, and X. Cai, PACIAE 2.0: An Updated parton and hadron cascade model (program) for the relativistic nuclear collisions, *Comput. Phys. Commun.* **183**, 333 (2012), [arXiv:1104.1238 \[nucl-th\]](#).
- [37] T. Sjostrand, S. Mrenna, and P. Z. Skands, PYTHIA 6.4 Physics and Manual, *JHEP* **05**, 026, [arXiv:hep-ph/0603175](#).
- [38] B. L. Combridge, J. Kripfganz, and J. Ranft, Hadron Production at Large Transverse Momentum and QCD, *Phys. Lett. B* **70**, 234 (1977).
- [39] R. D. Field, *Application of perturbative QCD* (Addison-Wesley Publishing Company, Inc., 1989).
- [40] The ALICE muon spectrometer covers negative pseudorapidity. However, in symmetric Pb+Pb collisions, positive values of rapidity are conventionally used for the muon coverage.
- [41] Z. Conesa Del Valle, *Performance of the ALICE muon spectrometer. Weak boson production and measurement in heavy-ion collisions at LHC*, Ph.D. thesis, Nantes U. (2007).